Disturbance Impulse Effects on Large Umbrella Space Reflector Dynamics

Sergey Belov[1, a)], Andrey Zhukov[1, b)], Mikhail Pavlov[2, c)] and Sergey Ponomarev[1, d)]

[1]*National Research Tomsk State University, 36 Lenin Avenue, Tomsk 634050 Russian Federation*
[2]*National Research Tomsk Polytechnic University, 30 Lenin Avenue, Tomsk 634050 Russian Federation*

[a)] corresponding author: belovsv@niipmm.tsu.ru
[b)]zh@niipmm.tsu.ru
[c)] mspavlov@tpu.ru
[d)]psv@niipmm.tsu.ru

Abstract. Large umbrella space antennas are essential for communication, monitoring and observation of Earth and space objects. Despite investigations devoted to space antenna dynamics, the disturbance impulse shape effect on the root mean square error of spacecraft antenna reflecting surface has not been studied. This paper overcomes this gap describing disturbance impulse impact on root mean square error of spacecraft antenna reflecting surface relative to paraboloid via nonlinear finite element method. Based on numerical results root mean square dependency on disturbance time for rectangular and sine impulses was calculated. This approach could be applied in studying antenna reflecting surface response on disturbance impulse for different types of perspective large space antennas.

INTRODUCTION

Large space parabolic antennas (LSPA) or space reflectors (with aperture 12 m and more) are vital for mobile communication, meteorological monitoring tools, observation of Earth and space objects. Such antennas have high gain and provide highly frequent wide-band signal transmission. In fully deployed state LSPA involve large cable stayed-shell structures. Their reflecting surface is a thin conductive molybdenum wire mesh with diameters part of millimeter and coated by gold (for example, AstroMesh antenna) [1]. The reflecting surface should be as close as possible to paraboloid surface to achieve improved radiotechnical parameters such as gain [2].

Integral qualitative geometrical parameter of reflecting surface is root mean square (RMS) error being related to the paraboloid surface

$$RMS = \sqrt{\frac{1}{S_a}\iint\limits_{S_a} \Delta z^2 dS}, \qquad (1)$$

where, Δz – reflecting surface deflection on paraboloid in direction of its axis; S_a – reflector aperture area.

Permissible RMS should be near 2% of operation wavelength [3]. There are works dedicated to space antennas but one of the most interesting is [4] where both fundamental methodologies of space antenna design and detailed review of antenna designs for some popular applications are presented. Despite the previous works devoted to space structures designing [5-7], the disturbance impulse shape impact on RMS error of spacecraft reflecting surface has not been described. This paper overcomes this gap describing disturbance impulse impact on RMS error of reflecting surface relative to paraboloid via nonlinear finite element method [8,9].

Prospects of Fundamental Sciences Development (PFSD-2016)
AIP Conf. Proc. 1772, 060001-1–060001-7; doi: 10.1063/1.4964581
Published by AIP Publishing. 978-0-7354-1430-3/$30.00

SPACECRAFT DESCRIPTION UNDER OPERATING SYSTEM DISTURBANCES

Spacecraft with large umbrella reflector includes block, solar panel, reflector and connecting bar (Figure 1).

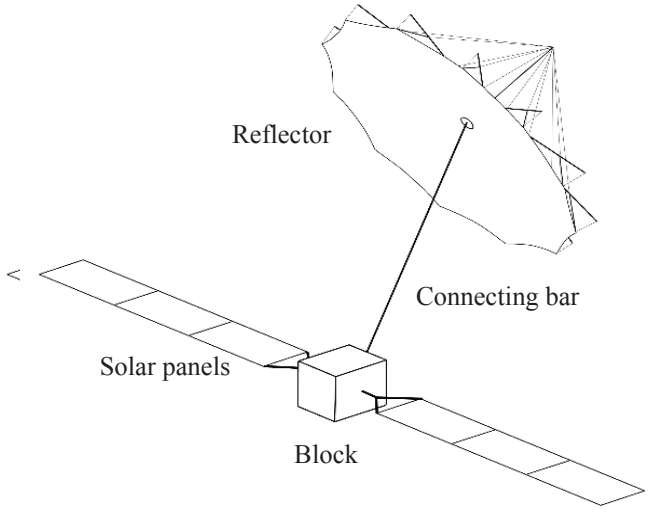

FIGURE 1. Spacecraft structure

The larger the geometrical spacecraft size is, the lower its stiffness level. Under conditions of existing operating system, disturbances generate oscillations. Such oscillations can produce focal point (feed) deflection relative to feed system, as well as deforming the reflector surface, which in its turn, result in operating break down.

PROBLEM STATEMENT

In Cartesian coordinates (x_1,x_2,x_3) spacecraft involves the spatial domain $\Omega(t)$ with boundary $\partial\Omega(t)$. Domain $\Omega(t)$ includes volumetric, shell and linear structures and embraces continuum determining specific material physico – mechanical properties as a coordinate function. Continuum point is characterized by vector $\mathbf{x}=\{x_1, x_2, x_3\}$.

Non-stationary solid mechanics governing equations, including elementary volume motion law, strain tensor and Hooke law describe spacecraft motion:

$$\rho\ddot{u}_i = \frac{\partial}{\partial x_k}\left(\sigma_{kj}\left(\delta_{ij} + \frac{\partial u_i}{\partial x_j}\right)\right), \tag{2}$$

$$\varepsilon_{ij} = \frac{1}{2}\left(\frac{\partial u_i}{\partial x_j} + \frac{\partial u_j}{\partial x_i} + \frac{\partial u_l}{\partial x_i}\frac{\partial u_l}{\partial x_j}\right), \tag{3}$$

$$\sigma_{ij} = \sigma_{ij}(\varepsilon_{lm}), \tag{4}$$

with initial conditions:

$$\begin{aligned} &\mathbf{u}(t=0,\mathbf{x}) = \mathbf{u^0}(\mathbf{x}), \\ &\dot{\mathbf{u}}(t=0,\mathbf{x}) = 0, \end{aligned} \quad \mathbf{x} \in \Omega(t) \tag{5}$$

as well as boundary conditions:

$$n_k\sigma_{kj}\left(\delta_{ij} + \frac{\partial u_i}{\partial x_j}\right) = p_i^n(t,\mathbf{x}), \ \mathbf{x} \in \partial\Omega(t) \tag{6}$$

where, u_i, σ_{ij}, and ε_{ij} – displacement vector components, second Piola-Kirchhoff stress tensor, strain tensor respectively; p_i^n – boundary stress characterized by normal vector $\bar{n}$. Hook law (4) is applied as:

$$\sigma_{ij} = \frac{E}{1+\nu}\cdot(\varepsilon_{ij} + \frac{\nu}{1-2\nu}\cdot\delta_{ij}\varepsilon_{ll}) - \frac{E}{1-2\nu}\cdot\varepsilon_{ij}^T\cdot\delta_{ij} + \sigma_{ij}^0 \tag{7}$$

where, E, ν – modulus of elasticity and Poisson's ratio of the material; ε_{ij}^{T} - thermal strain; σ_{ij}^{0} - initial tensor stress. Applying Hook law (7) is discussed in [10].

When t=0, the reflector is in initial stress-strain state for equations (2)-(6). Determining initial conditions of reflector stress-strain state is described in [11].

DISTURBANCES TYPES

To identify the reflector surface reaction a moment of impulse M_p was applied to spacecraft satellite block

$$M_p = \int_0^{\Delta t_{imp}} M_f(t)dt \tag{8}$$

where M_f – moment of force applied to spacecraft satellite block; Δt_{imp} - disturbance time.

Two function patterns were considered in coordinates $\left(t, M_f\right)$: rectangular impulse

$$M_f^{(1)}(t) = \begin{cases} A_1, & 0 \le t \le \Delta t_{imp} \\ 0, & t > \Delta t_{imp} \end{cases} \tag{9}$$

and sine impulse

$$M_f^{(2)}(t) = \begin{cases} A_2 \cdot \sin(\pi \cdot t / \Delta t_{imp}), & 0 \le t \le \Delta t_{imp} \\ 0, & t > \Delta t_{imp} \end{cases} \tag{10}$$

where, A_1 and A_2 – moment force impulse amplitudes defined by the following conditions

$$M_p^{(1)} = M_p^{(2)} = 10 \text{ N} \cdot m \cdot \text{sec}$$

Figure 2 shows the two function patterns – rectangular and sine disturbance which involve identical moment of impulse, according to (8)

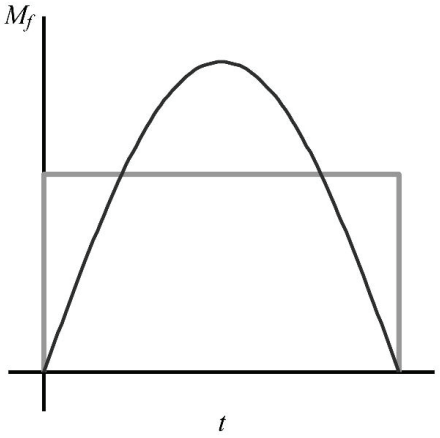

FIGURE 2. Rectangular and sine patterns of identical moment of impulse on spacecraft block

RESULTS AND DISCUSSION

The above stated problem is resolved by finite element method. Finite element of spacecraft model includes: total mass of 2500 kg; umbrella reflector mass of 65kg; reflector diameter of 12m; solar panel span of 30m with corresponding mass of 200kg; first bending oscillation frequency of solar panel is 0.07Hz; reflector surface tension – 5N/m. Moment of force vector M_f directionally normal to spacecraft symmetry plane. Self-damping of spacecraft structure is supposed to be small.

Relative RMS_{rel} error is applied as dynamic parameter for deflected reflecting surface from its optimum operating position. RMS_{rel} error is defined as:

$$\mathrm{RMS}_{\mathrm{rel}}(t)=\frac{\mathrm{RMS}(t)}{\mathrm{RMS}(t=0)}$$

where, $\mathrm{RMS}(t)$ - value in time; $\mathrm{RMS}(t=0)$ initial value. $\mathrm{RMS}(t)$ and $\mathrm{RMS}(t=0)$ are defined to (1). RMS_{rel} dependency to t for rectangular disturbance is depicted in Figure 3.

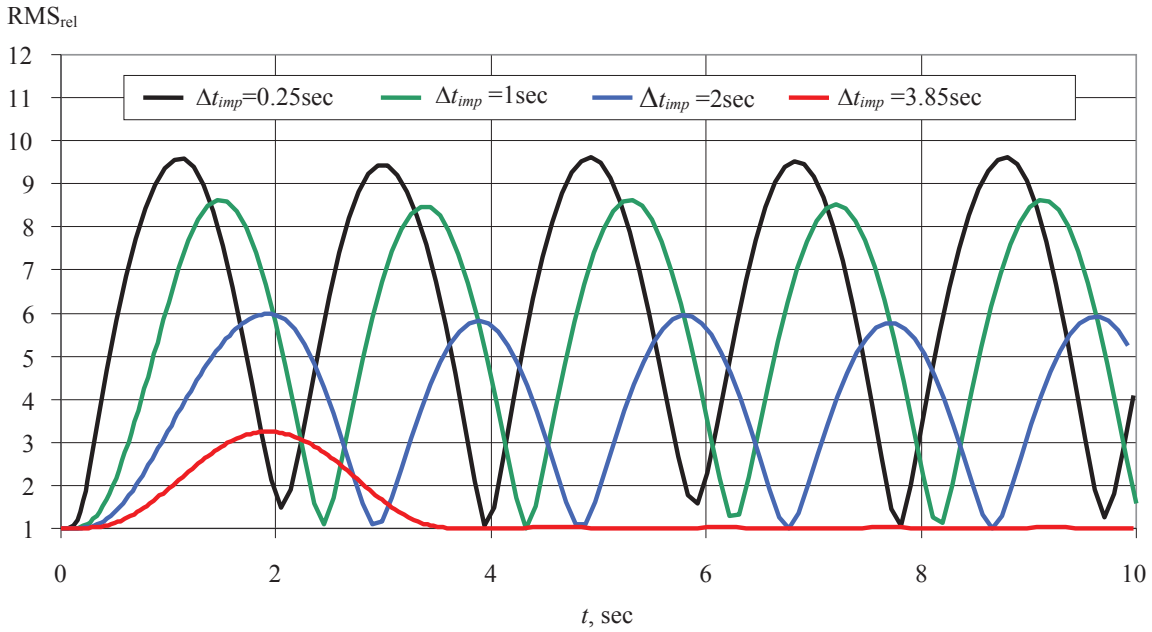

FIGURE 3. $\mathrm{RMS}_{\mathrm{rel}}(t)$ dependency for rectangular disturbance impulse

Figure 4 shows analogous dependency for sine disturbance.

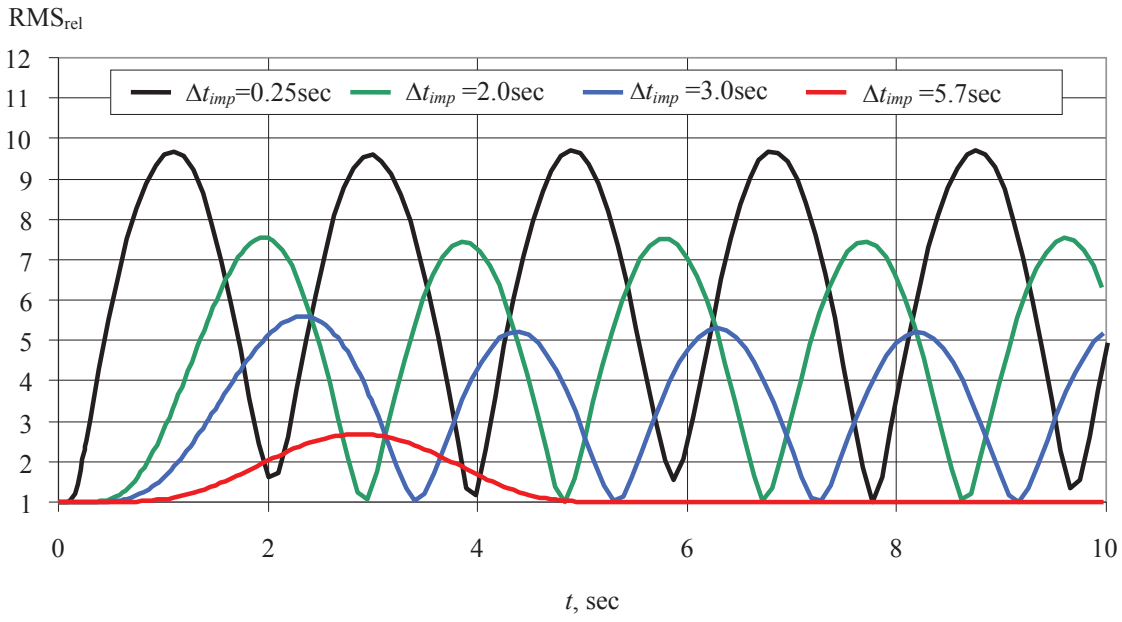

FIGURE 4. $\mathrm{RMS}_{\mathrm{rel}}(t)$ dependency for rectangular sine impulse

According to obtained results, spacecraft structure oscillations are excited by disturbance impulses within a period of T=3.85sec, which corresponds to the self-oscillation of the spacecraft (Figure 5).

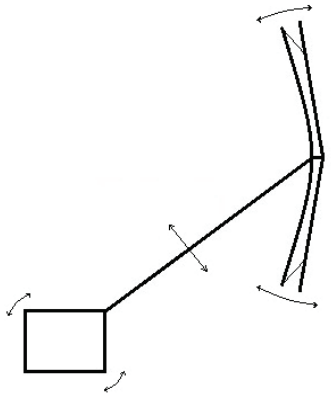

FIGURE 5. Excited shape after disturbance impulse

After disturbance impulse interference, spacecraft oscillations continue (i.e. residual oscillations (RO)). RO amplitude decreases while disturbance impulse time Δt_{imp} increases. This could be explained by the fact that amplitudes A_1 and A_2 in (9) and (10) decrease. RO could vanish if disturbance impulse time is consistent to excited oscillation period. In the case of rectangular disturbance impulse, RO are not observed (Fig.3) if disturbance impulse time equals to oscillation period ($\Delta t_{imp}=T$). In the case of sine disturbance impulse (Fig.4) the above-mentioned effect is evident, when Δt_{imp} =1.5 T.

Spacecraft structure oscillations are excited if

$$\frac{dM_f}{dt} \neq 0 \tag{11}$$

If $\frac{dM_f}{dt} = 0$, then static load is additionally distributed. Condition (11) is satisfied, if rectangular disturbance impulse is applied in t=0 and t=Δt_{imp}. In this case oscillations are excited which are identical in shape and different in sign. If the phase difference between oscillations is 2π-fold, then RO fade away. In case of sine disturbance, (11) is satisfied throughout disturbance time itself. Such a situation is much more complicated for qualitative analysis. However, in this case, no RO could be explained by the corresponding phase changes. RO amplitudes RMS_{rel}^{amp} vary depending on impulse disturbance times as seen in Figure 6.

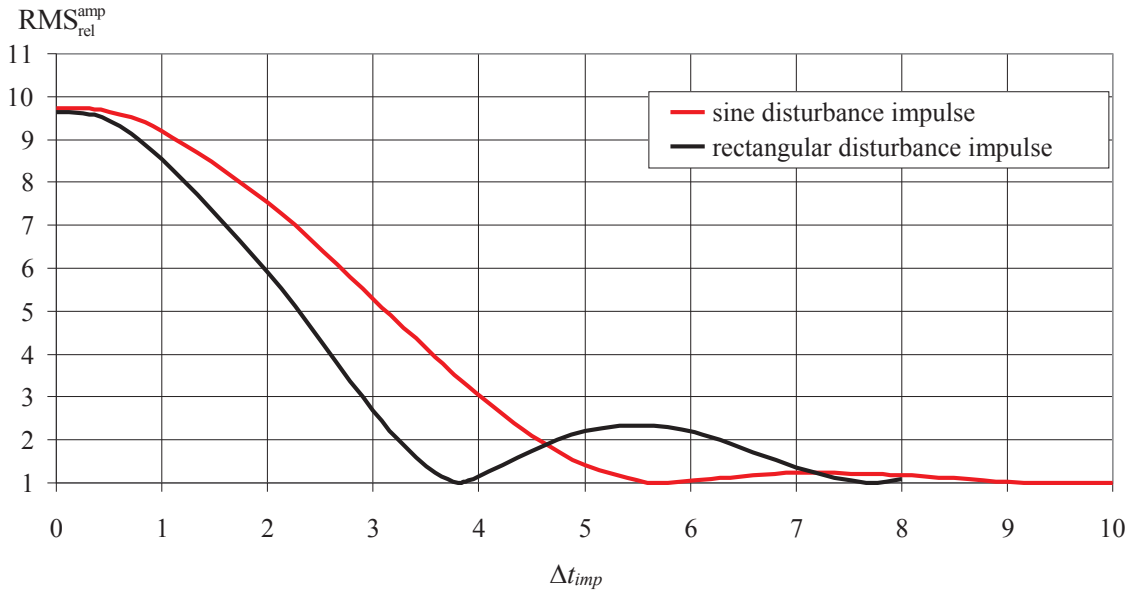

FIGURE 6. RMS_{rel}^{amp} residual oscillation amplitudes depending on impulse disturbance time

According to represented results, it should be noted that RO amplitudes are independent not only of short impulse disturbance times (Δt_{imp} <0.5 sec), but also of disturbance type. This could be explained by the fact that given moment of impulse to spacecraft block involves short-time disturbance, and this disturbance itself does not expand quickly enough throughout the spacecraft structure elements. It could be considered that the moment of impulse is imposed to the spacecraft immediately.

Increasing disturbance time Δt_{imp} results in decreasing oscillations amplitudes, which, in its turn, attain the first minimum. Another situation is when oscillation amplitudes increase and then decrease, attaining second minimum. RMS_{rel} dependency to t, when Δt_{imp} corresponds to the second minimum, is depicted on Figure 7.

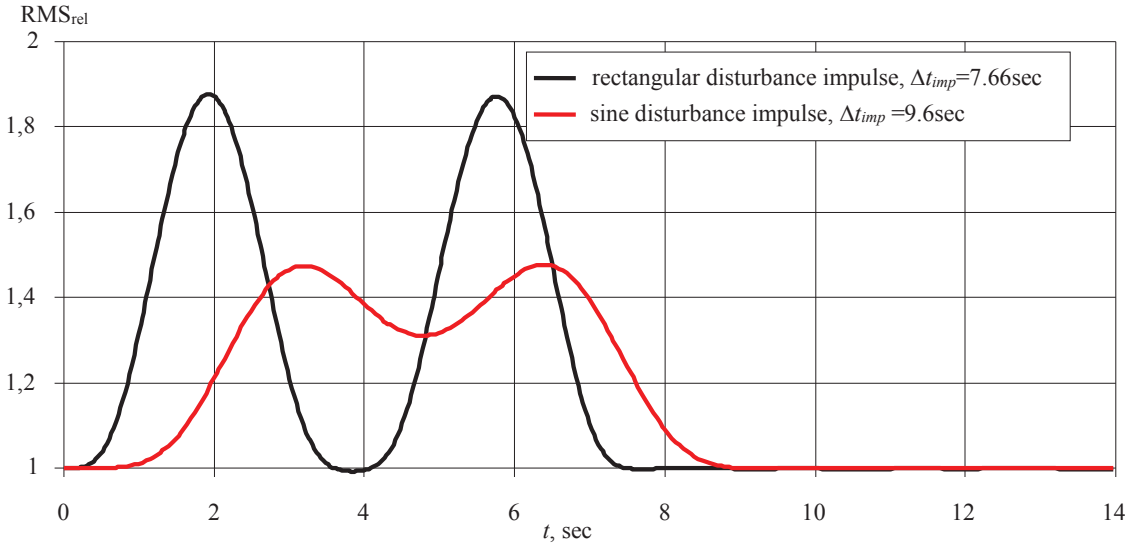

FIGURE 7. RMS_{rel} dependency to t, when Δt_{imp} corresponds to the second minimum RMS_{rel}^{amp}

Under the condition when Δt_{imp} increases, one can observe minimum function sequences which correspond to time step T=3.85sec. The difference is related to first minimum locations. In case of rectangular disturbance impulse the first minimum is positioned in point $\Delta t_{imp} = T$, when sine impulse disturbance it is in point $\Delta t_{imp} = 1.5T$.

CONCLUSION

The present paper discussed the numerical analysis of umbrella reflector dynamics when spacecraft is affected by rectangular and sine disturbance impulses. It was determined that corresponding reflector surface response was identical for both types of disturbance. Adjustment of disturbance time Δt_{imp} to excited oscillation period minimizes RO amplitudes. There is a disturbance time Δt_{imp} sequence, where RO amplitudes show minimum. On time axis Δt_{imp} minimum points are positioned, as the step is equal to excited oscillation period. Disturbance type affects relative position of the first minimum.

ACKNOWLEDGMENTS

This work has been financially supported by Ministry of Education and Science of the Russian Federation. Unique identifier RFMEFI57814X0073.

REFERENCES

1. S. Morterolle, B. Maurin B., J. Quirant. and C. Dupuy, Acta Astronaut. **76** , 1, 154-163 (2012).
2. G. Tibert, "Deployable tensegrity structures for space applications", Ph.D. thesis, Royal Institute of Technology, 2002.

3. J. Du, Y. Zong and H. Bao, Aerosp. Sci.Technol. **30**, 26–32 (2013).
4. W. A. Imbriale, S. S. Gao and L. Boccia, *Space Antenna Handbook* (John Wiley & Sons, Ltd, West Sussex, 2012), pp.17-17.
5. G. S. Nurre, R. S. Ryan, H. N. Scofield and J. L. Sims, J. Guid. Control Dynam., **7**,5, 514–526 (1984).
6. Q. Hu and P. Shi, J. Guid. Control Dynam., **30**, 3, 804−815 (2007).
7. K. Tsuchiya, J. Guid. Control Dynam., **6**, 2, 100−103 (1983).
8. P. Wriggers, *Nonlinear Finite Element Methods* (Springer, Berlin, Heidelberg, 2008), pp.205-223.
9. J. N. Reddy *An Introduction to Nonlinear Finite Element Analysis*, (Oxford University Press, New York 2004), pp.287-296.
10. A. P Zhukov, and S. V Ponomarev (in Russian - Zhurnal Izvestia vuzov. Fizika, Tomsk) **12/2**, 118-124 (2010).
11. S. Ponomarev, A. Zhukov, A. Belkov, V. Ponomarev, S. Belov and M. Pavlov, IOP Conf. Ser.: Mater. Sci. Eng. **71**, 012070 (2015), available at http://iopscience.iop.org/article/10.1088/1757-899X/71/1/012070/pdf.